Operation and Expected Performance of the NLC Main Linacs*

Ralph W. Assmann and Tor O. Raubenheimer
Stanford Linear Accelerator Center, Stanford University, Stanford, CA 94309

ABSTRACT

The main linacs for the proposed Next Linear Collider (NLC) provide acceleration of up to 500 GeV per beam. The linacs operate in a regime where unavoidable imperfections and even natural ground motion cause significant emittance dilutions. In order to achieve the NLC luminosity goals, small emittance beams must be transported with an emittance growth of less than about 175% for the 1 TeV center-of-mass version of the NLC. In this paper we discuss the operation and the expected performance of the NLC main linacs. Under the assumption that the specified device tolerances are met, it is shown from detailed simulations that the linac emittance transport fulfills the NLC requirements.

I. INTRODUCTION

The design of the NLC main linacs is described in [1]. Here we discuss numerical calculations that were performed to study the operation and expected performance of the NLC main linacs in greater detail. By assuming realistic errors in all major accelerator components, we can study the complex interactions between different mechanisms of emittance growth and the proposed correction algorithms. Since stability problems are of major concern for the NLC, we also discuss simulation results for the alignment stability in the NLC main linacs.

The results that are presented here were obtained by using the simulation program LIAR [2]. This program is used both for the existing Stanford Linear Collider (SLC) and the proposed NLC. Assuming realistic imperfections, LIAR predicts an emittance growth for the SLC that is in agreement with the experimental observation. This benchmark result gives us confidence that the emittance dilution for the NLC can be estimated with an accuracy of better than 50% for given rms accelerator errors.

II. SIMULATION PARAMETERS

The NLC tolerances are tighter for the larger bunch currents and the longer bunch lengths at higher beam energies. Therefore we restrict this study to the 1 TeV center-of-mass version of NLC (NLC-IIb). The corresponding beam parameters are listed in Table II. The full NLC-II lattice was used for the simulations. Disturbances from the NLC diagnostics stations and imperfections of the multibunch beam loading compensation were not considered. Beam-induced short-range and long-range wakefields were described by parameterizations that were obtained from detailed calculations [1, 3, 4]. It is important to note that recent experiments [5] have shown excellent quantitative agreement between measured and calculated wakefields for the NLC.

*Work supported by the Department of Energy, contract DE-AC03-76SF00515

Parameter	Value
Bunches in train	90
Bunch population	1.1×10^{10}
Repetition frequency	120 Hz
Gaussian bunch length	150 μm
Rf frequency	11.424 GHz
Unloaded gradient	85 MV/m
Multibunch loading	-21.5 MV/m
Single-bunch loading	-0.5 MV/m
Injection energy	10 GeV
Injection energy spread	1.5%
Inj. hor. emittance $\gamma\epsilon_x$	3.6×10^{-6} m-rad
Inj. vert. emittance $\gamma\epsilon_y$	4.0×10^{-8} m-rad
Final beam energy	500 GeV

Table I: Accelerator parameters for the 1 TeV center-of-mass version of NLC (NLC-IIb).

Component	Number	Error source	Rms error
Quadrupoles	729	Alignment	100 μm
		Roll	300 μrad
		Gradient	0.3%
Rf structures	4908	Phase	1°
		Gradient	0.2%
Quad. BPM's	728	Alignm. in quad.	2 μm
		Resolution	1 μm
Struc. BPM's	9816	Alignm. in struc.	15 μm
Feedbacks	7	-	-
Mover points	3183	-	-
Dipole corr.	729	-	-

Table II: Type and number of beamline components and associated error sources per NLC linac. We only list components that are relevant for the tuning of the main linac. The assumed rms errors are specified.

A list of beamline components that are relevant for the tuning of the main linacs is shown in Table II. We assume that all listed components are available and perform within their expected rms errors. We do not consider the effects of unavailable BPM's or magnet movers. Reliability requirements are studied in a working group that was recently set up at SLAC. The small initial emittance in the vertical plane exhibits a large sensitivity against accelerator imperfections. We therefore restrict this study to the vertical plane.

Config	ϕ_1 [°]	E_1 [GeV]	ϕ_2 [°]	E_2 [GeV]	ϕ_3 [°]	E_{overhead} [%]
1	4	30	-7	485	-30	0.2
2	8	30	-5	455	-30	0.7
3	10	30	-3	425	-30	1.3
4	12	30	-1	400	-30	2.0
5	14	30	1	380	-30	2.6
6	16	30	3	360	-30	3.2
7	18	30	5	335	-30	4.1
8	20	30	7	320	-30	4.8
9	22	30	9	300	-30	5.7

Table III: BNS configurations: ϕ_1, ϕ_2 and ϕ_3 are the three Rf phases in the linac and E_1 and E_2 are the switching points. each BNS is characterized by the energy overhead E_{overhead}.

III. BNS DAMPING

The main linacs of the NLC operate in a regime where beam-generated wakefields can cause significant emittance growth. As the head of a bunch enters off-center into an accelerating Rf structure, dipole wakefields are excited and the tail of the bunch is deflected. The differential deflection along the bunch increases the projected horizontal and vertical emittances. Beam-based alignment is used to minimize the static offset between the beam and the Rf structures (compare section IV). However, incoming coherent betatron oscillations also cause offsets between the beam and the Rf structures. The resulting wakefields add up resonantly and can cause large emittance growth. BNS damping [6] is used to minimize this effect. We assume that there is no correlation between particle energy $E(z)$ and longitudinal position z at injection:

$$E(z) = \text{const} \qquad \text{for all } z\,. \tag{1}$$

The coordinate z describes the longitudinal position within a bunch. Two effects introduce E-z correlations in the linac:

1. The head of the bunch excites *short-range longitudinal wakefields* that decelerate all subsequent particles. This effect is called *single-bunch loading*. It depends on the bunch length, shape, charge and the Rf structures.

2. Due to the curvature of the accelerating Rf, different particles along the bunch see slightly different accelerating gradients. This effect can be enhanced if the bunch arrives before or after the crest of the Rf. The tail of the bunch sees more or less acceleration than its head. The delay between the bunch and the Rf crest is specified as the *Rf phase*.

An incoming coherent betatron oscillation causes dispersion. The E-z correlation therefore produces a differential deflection along the bunch. In addition chromatic errors apply. BNS damping is implemented by adjusting the E-z correlation such that dispersive and chromatic errors compensate the differential transverse wakefield deflection. This is realized by changing the Rf phases along the linac.

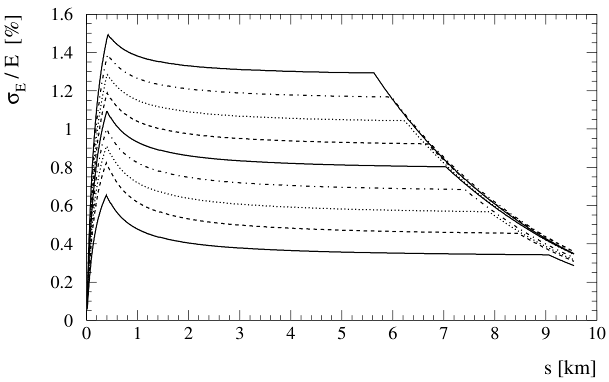

Figure 1: Beam rms energy spread along the linac for different BNS configurations. The energy spread was set to zero at the start and was fixed to about 0.3% at the end, as required by the final focus system. The different BNS configurations are defined in Table III and are referred to as number 1 to 9, where 1 is the lowest curve.

In order to identify an optimal BNS configuration we studied a number of energy spread profiles along the linac, each of which is generated by adjusting the Rf phases in three groups. The BNS configurations number 1 to 9 are defined in Table III. All BNS cases were calculated to give the required final beam energy spread of about 0.3% rms. Table III characterizes the different BNS configurations in terms of the energy overhead required to generate them. The energy overhead is defined as the relative difference between the final beam energy E_0, obtained with the nominal average Rf phase, and the final beam energy E_{bns}, obtained with the BNS Rf phases:

$$E_{\text{overhead}}[\%] = 100 \cdot \left(1 - \frac{E_0}{E_{\text{bns}}}\,.\right) \tag{2}$$

From now on we refer to the BNS cases by their energy overhead. To study BNS in terms of emittance preservation, we simulated the emittance growth for an initial 1σ vertical beam offset (2.2 μm). The initial uncorrelated beam energy spread was set to zero. As shown in Figure 2, we find the smallest emittance growth for a BNS energy overhead of 1.3%. Wakefields cause large emittance growth for lower energy overheads while dispersive emittance growth is important in the opposite direction. An energy overhead of 1.3% is well inside the NLC specification of up to 3% and we chose this BNS scheme for all further studies. Depending on the different functional dependencies, the combination of the curvature of the Rf and single-bunch beam loading can lead to a situation where the core of the bunch is BNS damped but the tail is not or is even anti-damped. In this case a significant beam tail could be generated. It was verified that BNS damping is effective for the whole NLC bunch.

The emittance growth with optimum BNS and a 1σ initial offset error is about 4%. However, it becomes roughly 40% if the initial uncorrelated energy spread of 1.5% is included. The initial energy spread significantly changes the beam dynamics

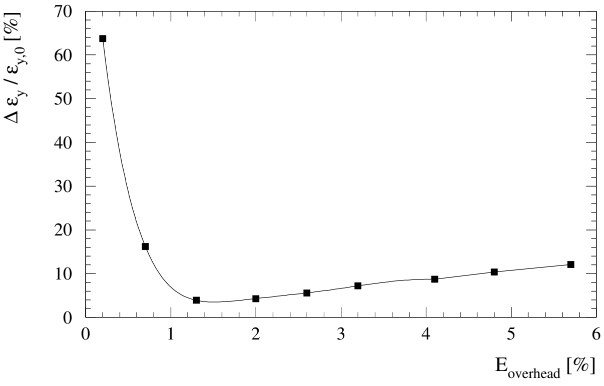

Figure 2: Average vertical emittance growth $\Delta\epsilon_y/\epsilon_{y,0}$ for the different BNS configurations from Figure 1 and a 1σ (2.2 μm) initial beam offset. The initial uncorrelated beam energy spread was set to zero.

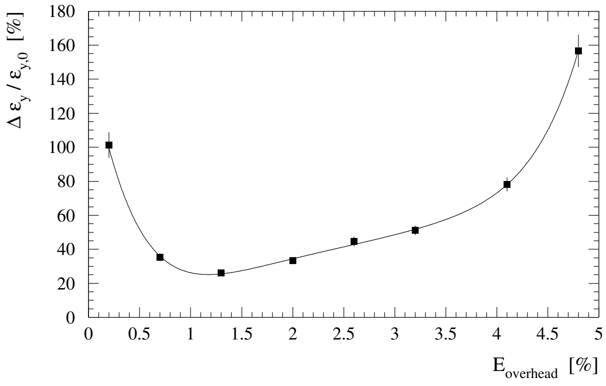

Figure 3: Average emittance growth $\Delta\epsilon_y/\epsilon_{y,0}$ after beam-based alignment for different BNS configurations. We used an initial quadrupole alignment of 50 μm rms, a static BPM to quadrupole offset of 2 μm rms, a BPM-resolution of 1 μm rms and perfect structure BPM's. The alignment was done in 14 sections and 5 iterations.

in the beginning of the linac. It causes dispersive filamentation and finally sets the injection tolerances.

IV. BEAM-BASED ALIGNMENT

Initial misalignments in the NLC linacs are large compared to the final tolerances. Therefore the "conventional" alignment must be complemented by beam-based alignment techniques. The linac emittance growth is driven by transverse offsets between the beam and the centers of quadrupoles and Rf structures. Those offsets must be minimized in order to maintain the normalized emittances. The beam-based alignment algorithm for the NLC linacs is described in [7]. Here we shortly summarize the main results.

Assuming that all beam deflections are caused by the quadrupoles, N BPM measurements were used to solve for N-2 quadrupole offsets and the initial offset y and angle y' of the beam. The positions of the first and last quadrupole in a corrected section were fixed. The endpoint BPM's defined the reference line for the alignment. The quadrupoles were aligned non-disruptively to the NLC operation with magnet movers at each quadrupole support. Problems from the finite step size of the magnet movers ($\approx$0.25 μm) were assumed to be avoided by having a dipole corrector at each quadrupole. Small quadrupole misalignments should be corrected by shifting the effective magnetic center. If the dipole strengths get large enough they can be "exchanged" for a step of the quadrupole mover. Because the alignment model is perturbed by wakefields and imperfections, the alignment solution was iterated and interleaved with the alignment of the Rf structures.

The Rf accelerator structures have a structure BPM at each end. Two Rf structures are always mounted on a single support structure. Every support structure can be moved by stepping motors at either end. The structures were aligned by adjusting the movers such that the average structure BPM reading on a girder was minimized. The Rf structure alignment was performed after each iteration of quadrupole beam-based alignment.

We now discuss an NLC simulation where the quadrupole BPM's had a 2 μm rms static offset with respect to the quadrupoles and a 1 μm rms resolution. The initial quadrupole misalignment was 50 μm rms and the structure BPM's had no imperfections. The alignment was done in 5 iterations. Figure 3 shows the resulting average single-bunch emittance growth for the different BNS. As before, BNS configuration 3 yields the smallest emittance growth. This demonstrates the importance of the right choice of Rf phases for beam-based alignment. The minimal emittance growth of 28% results mainly from the errors of the quadrupole BPM's.

However, we did not yet include all relevant imperfections. Using the quadrupole rms misalignment and all quadrupole and structure BPM errors from Table II we find an emittance growth of $(90.2 \pm 6.0)\%$ after beam-based alignment. The major sources of emittance dilution in this case are the errors in the structure BPM's. This emittance growth is well below the 175% requirement in the NLC design.

V. LONG-RANGE WAKEFIELDS

Thus far, we have only considered single-bunch effects. Now we include the whole bunch train of 90 bunches and transverse long-range wakefields. Figure 4 shows the effect of a 1σ offset of the injected beam. Both single bunch and multibunch wakefields were included. The emittance of the first bunch grows by 38.7%, the average single bunch emittance growth is 49.0% and the total emittance growth is 54.4%. The difference between the last two numbers reflects the impact of the long-range transverse wakefields. The emittance growth is clearly dominated by single-bunch wakefield effects.

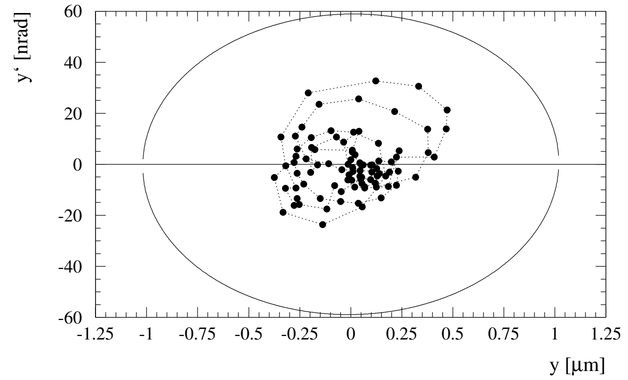

Figure 4: Phase space locations y and y' of the bunches at the end of the linac for a 1σ initial vertical beam offset. y and y' are referenced to their average values. The bunch positions are compared to the beam ellipse from the average single-bunch emittance.

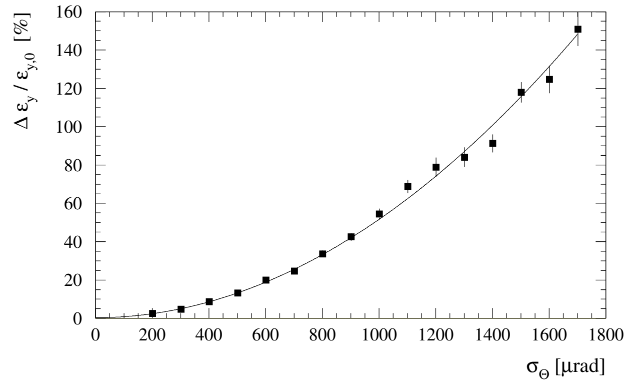

Figure 5: Vertical emittance growth $\Delta\epsilon_y/\epsilon_{y,0}$ as a function of the rms quadrupole roll θ around the longitudinal direction.

VI. BETATRON COUPLING

The horizontal emittance in the NLC main linacs is about 100 times larger than the vertical emittance. Betatron coupling can couple part of the horizontal emittance into the vertical plane. We studied the effect of emittance coupling without any trajectory offsets. Figure 5 shows the simulated growth of the vertical emittance as a function of the rms quadrupole roll. For a roll of 300 μrad rms, the emittance growth is well below 10% and is not important.

VII. TOTAL EMITTANCE GROWTH

The emittance growth of a 90 bunch NLC beam including all accelerator errors from Table II and after beam-based alignment was simulated to be

$$\Delta\epsilon_y/\epsilon_{y,0} = (106.6 \pm 3.9)\% \tag{3}$$

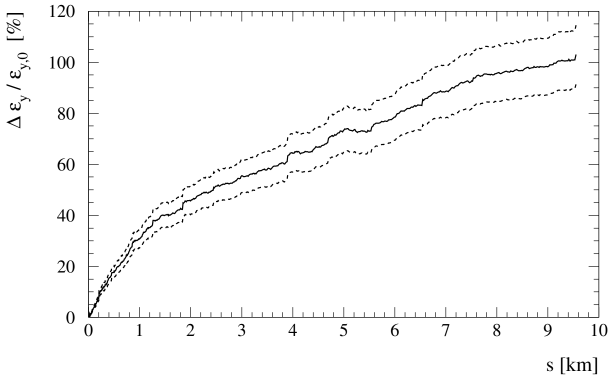

Figure 6: Average emittance growth $\Delta\epsilon_y/\epsilon_{y,0}$ along the linac for the full simulation. The dashed curves specify the error-bands around the average (solid curve).

from 200 different error distributions. This number is well below the 175% requirement in the NLC design. Internal structure misalignments, special multibunch imperfections and the effects of missing BPM's were not included but are being studied. Preliminary results show that the emittance growth might increase by an additional 20-30%.

Figure 6 shows the average emittance growth along the linac for 100 seeds of the full simulation. The growth shows roughly a square-root dependence on the longitudinal position s. No particularly bad region can be identified. Very small residual step increases of the emittance were caused by the transitions between alignment sections.

VIII. ALIGNMENT STABILITY

The alignment stability determines how often beam-based alignment must be applied. Emittance growth due to slow alignment drifts is mainly caused by quadrupole movements. We do not discuss BPM stability in detail. However, the requirements are tight. We assumed a 2 μm static rms offset between the BPM and quadrupole centers. This can be achieved with a beam-based procedure and must be stable over significant periods of time (days).

In order to model alignment drifts we used the ATL-model [8]. It predicts the rms vertical misalignment $\sigma_{\Delta y}$ (in μm) with time T (in seconds) and over the length L (in m):

$$\sigma_{\Delta y}^2 = A \cdot T \cdot L\,. \tag{4}$$

The coefficient A was measured to be smaller than $5 \times 10^{-7} \mu\mathrm{m}^2$/s/m in the temperature-stabilized FFTB tunnel at SLAC [9]. Note that this measurement of A was done over 150 hours for quadrupoles in a real beamline environment. In order to be conservative, we used the FFTB upper bound value of $5 \times 10^{-7} \mu\mathrm{m}^2$/s/m for our study. Details are described in [10]. Assuming a perfect starting point (flat trajectory, no emittance growth) we simulated the alignment drift and calculated the deterioration of the trajectory and the emittance. The emittance

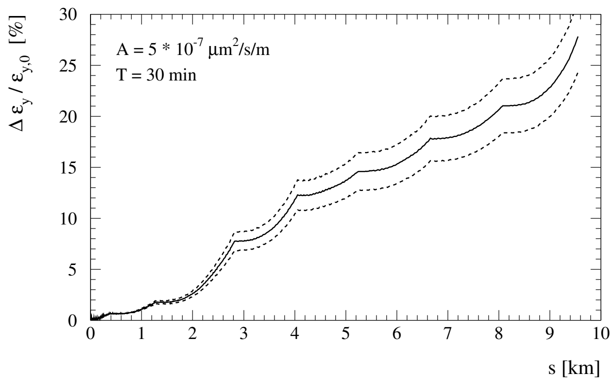

Figure 7: Average vertical emittance growth $\Delta\epsilon_y/\epsilon_{y,0}$ along the linac for ATL-like drifts after 30 minutes. The dashed curves specify the errorbands around the average.

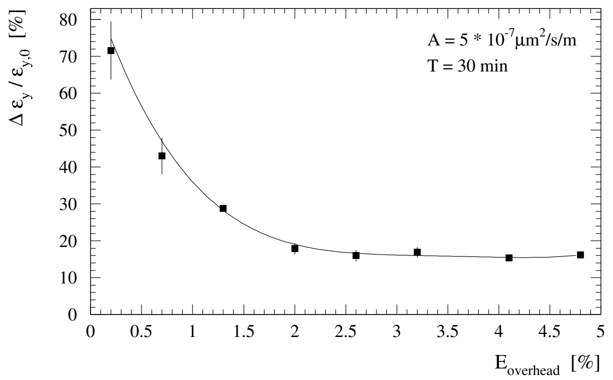

Figure 8: Average vertical emittance growth $\Delta\epsilon_y/\epsilon_{y,0}$ from ATL-like alignment drifts for different BNS configurations.

growth was found to be:

$$(54.0 \pm 1.6)\% \quad \text{per hour.}$$

This number must be added roughly in quadrature to the static emittance growth of 107%. Beam-based alignment, that serves as an effective trajectory correction at the same time, needs to be done every 1/2 to 1 hour. Since it can be applied continually, this does not impose a major problem in the operation of the NLC linacs. The emittance growth along the linac after 30 minutes drift is shown in Figure 7. As a coherent betatron oscillation builds up the emittance starts to grow rapidly. Seven feedbacks limit this growth.

Figure 8 shows the average single-bunch emittance growth for different BNS configurations. BNS configurations with higher energy overheads reduce the emittance growth after 30 minutes of alignment drift from 29% to about 16%. One can therefore imagine to trade alignment performance against better stability.

IX. CONCLUSION

A concept for the operation and optimization of the main linacs for the Next Linear Collider (NLC) was described. Many aspects were studied: BNS damping, beam-based alignment, transverse long-range wakefields, betatron coupling and alignment stability. The simulations included multiple accelerator imperfections and were carried out with a computer program that has been benchmarked against the existing Stanford Linear Collider (SLC). We conclude that the small vertical emittance beams of NLC can be transported and accelerated in the main linacs with a growth in the normalized emittance that is smaller than the 175% design requirement. Assuming that all devices operate within their rms tolerances we calculated an average emittance growth of about 110%. Additional imperfections are expected to increase this number to about 130-140%. We showed that emittance deterioration due to alignment drifts can be handled by regular (hourly) maintenance of the beam trajectories. Future studies will consider more detailed tuning and reliability requirements.

X. ACKNOWLEDGMENTS

This work profited in many ways from the discussions with other members of the NLC linac design group: Chris Adolphsen, Karl Bane and Kathy Thompson. We also wish to thank Reinhard Brinkmann, Dave Burke and Bob Siemann for their useful comments.

XI. REFERENCES

[1] The NLC Design Group, “Zeroth-Order Design Report for the Next Linear Collider”, SLAC report 474 (1996).

[2] R. Assmann et al., “LIAR - A Computer Program for Linear Accelerator Simulations”, SLAC/AP-103 (1996).

[3] K. Bane and P. Wilson, Proc. of the 11^{th} Int. Conf. on High Energy Acc., CERN 1980, p. 592.

[4] N. Kroll, et.al., “Manifold damping of the NLC detuned accelerating structure”, SLAC-PUB-6660 (1994).

[5] R.H. Miller, et al., “A damped detuned structure for the Next Linear Collider”, Proc. LINAC96, Geneva, August 26-30, 1996. SLAC-PUB-7288 (1996).

[6] V. Balakin, A. Novokhatsky and V. Smirnov, “VLEPP: Transverse Beam Dynamics”, Proc. of the 12th Int. Conf. on High Energy Accelerators, Fermilab (1983).

[7] R. Assmann et al., “Emittance and trajectory control in the main linac of the NLC”, LINAC'96. SLAC-PUB-7301 (1996).

[8] V. Shiltsev, “Space-Time Ground Diffusion: The ATL Law for Accelerators”. Proc. of the 4^{th} IWAA95, Nov. 14-17, 1995, KEK, Japan. IV 352.

[9] R. Assmann, C. Montag and C. Salsberg, “Beamline stability measurements with a stretched wire system in the FFTB”, LINAC'96. SLAC-PUB-7303 (1996).

[10] R. Assmann et al., “Emittance dilution due to slow alignment drifts in the main linacs of the NLC”, LINAC'96. SLAC-PUB-7302 (1996).